Generalized dimer states: hierarchies

1994 J. Phys.: Condens. Matter 6 11099

(http://iopscience.iop.org/0953-8984/6/50/018)

J. Phys.: Condens. Matter 6 (1994) 11099–11117. Printed in the UK

Generalized dimer states: hierarchies

M W Long and C A Hayward
School Of Physics, Birmingham University, Edgbaston, Birmingham B15 2TT, UK

Received 20 June 1994, in final form 21 September 1994

Abstract. We present variational calculations for quantum spin-half models based upon modifications to nearest-neighbour dimer states. Using a sequence of projections we can attempt a sort of finite-size scaling, in the number of variational parameters, towards the exact solution. For the simple nearest-neighbour Heisenberg model we achieve an error of only 0.005% in energy for our most accurate calculation, much better than an equivalent Lanczos calculation, with which we compare. Due to the fact that we control the total spin in our wavefunctions, we can evaluate the coherence lengths associated with cyclic-exchange permutations (the spin-half sector) and for spin–spin correlations (the spin-one sector), yielding, for example, a convincing numerical confirmation that the spin-one biquadratic-exchange Hamiltonian has a finite correlation length. We perform a study of the one-dimensional J_1–J_2 model, trying to predict the onset of the phase transition by searching directly for the divergence of the correlation length. Our calculations predict the phase transition near $J_2/J_1 \sim 1/4$, as expected. We also perform a study of the ladder geometry, giving further evidence that infinitesimal coupling between ladders yields an immediate gap in the spectrum. The only complication is that the minimization over our space of variational parameters is subtle: surprisingly complicated and 'difficult to find' structure is observed in our low-energy solutions which might make our approach of limited use.

1. Introduction

The role of quantum mechanics in spin physics has captivated a generation of magnetism theorists. In 'high'-dimensional systems the classical solution reigns supreme, but in 'low'-dimensional systems any order is shaken apart by the low-energy collective excitations and a new, truly quantum mechanical state replaces the classically ordered state. It is to this quantum solution that the theorists have addressed themselves, trying to describe the phenomena to be expected in such a state.

The models which are used to describe low-dimensional magnetism can be chosen to be as simple as possible with hardly any reduction in difficulty. The elementary Heisenberg model is probably the best studied, and although the nearest-neighbour variant has been solved by Bethe *ansatz* [1], the solutions have to be interpreted in terms of spin-half and spin-one excitations [2], and the relative role of these excitations remains fairly obscure. When one adds next-nearest-neighbour coupling, leading to the J_1–J_2 model, in order to study the phase transition between the gapless $J_2 = 0$ and gapped $2J_2 = J_1$ phases [3], there is no exact solution to help and one is left to consider possible approximation schemes. We will develop such an approximation scheme in this article, extending the simplistic treatment previously suggested [4] to a rather higher level.

There are several methods of tackling quantum spin systems, all with their associated drawbacks. Firstly, one can go to the continuum limit and study the associated field theory [5]. The drawback with this approach is that the taking of this limit is not controlled and so the writing down of the model constitutes a guess. The strength of the technique

0953-8984/94/5011099+19$19.50

is that understanding the physics of the solution is 'easier'. Secondly, there is the trick of mapping the original hard-core boson problem onto an equivalent fermion problem, the so-called Jordan–Wigner transformation [6]. The hard-core constraint is dealt with by Pauli exclusion and then the weaker coherence effects can be approximated by mean-field theories. One weakness in this approach is that the mean-field approximation applied to the residual interactions is poor and 'ordered' solutions are greatly preferred over strongly correlated solutions. A second weakness is that any refinement requires a significant advance in treating the correlated fermionic problem, a very difficult task. Thirdly, one has exact diagonalization and quantum Monte Carlo techniques, which involve no inherent error but which require that the phenomenon investigated be observable in the rather small systems analysed. Finally, one has variational approaches which involve guessing sensible and accurate solutions to the problem at hand. Obviously, the great weakness of variational calculations is that they are uncontrolled and therefore cannot be assessed easily.

In this article we will develop a *sequence* of variational calculations which we believe converge to the *exact* answer. This allows us to perform a sort of 'finite-size-scaling' analysis in order to try to deduce the behaviour, in a very similar way to that employed in exact diagonalization. A second feature of our analysis is the ability to calculate *and interpret* the long-range properties of the correlation functions, allowing us to predict where and how the phase transition in the J_1–J_2 Heisenberg model occurs.

The key to our calculations is a non-orthogonal representation to the total-spin singlet subspace of the spin-half chain [7]. Although the basis is difficult to use, it has the advantage that *all* the conservation laws have been extracted and so states with perfect quantum numbers can be created. In simple terms, we start out with a pairwise dimerized state, and then by successive hierarchies of transpositions, we include more and more distant spin correlations. One might imagine that at each order the length of singlets is increased by one, but this is not directly true, since the non-orthogonality confuses the issue and makes the length of singlets a non-trivial concept. If we use the spin–spin correlations to define what we mean by length of singlets, then we construct states with correlation lengths of forty atoms, although the number of imposed transpositions is only six.

As a test of our scheme, we have elected to look at the spin-one biquadratic-exchange Hamiltonian, which can be solved exactly [8]. The point here is that the analytic correlation length is 21 atoms and so is unlikely to show up in an exact diagonalization analysis. We have little problem in obtaining evidence for the existence of a finite correlation length.

Our real interest, however, is in the phase transition found in the J_1–J_2 model. We apply our scheme to this model with the intention of both pinning down when the transition occurs and secondly trying to establish that the transition is controlled by the topological excitations in the system.

A second system of great current interest is the ladder geometry [9]. The issue in this system is when the phase transition between the gapless phase with uncoupled rails to the gapped phase with coupled rails occurs. Numerical evidence seems to suggest that infinitesimal coupling yields a gap [9], and our technique provides corroborative evidence.

In section 2 we introduce the calculational scheme, in section 3 we apply the technique to the total-spin-zero projector Hamiltonians, which include the biquadratic-exchange Hamiltonian as a special case, in section 4 we look at the J_1–J_2 Hamiltonian for spin-half, in section 5 we look at the ladder geometry, and in section 6 we conclude.

2. Hierarchical variational states and their correlation functions

The approach that we are developing revolves around the existence of a complete

representation to the total-spin-singlet subspace for spin-half atoms [7], which enables us to perform variational calculations with correct quantum numbers. We have provided a description of this representation in a previous article [4], but we will repeat the description here because it is an essential ingredient of an understanding of our calculations.

The basis we elect to use involves choosing two equal-sized sublattices of spins, combined with an order which alternates between sublattices. For the linear chain this choice is very natural and we shall use the obvious order along the chain in this article. The states in our basis then involve pairing up all the spins, with one from each pair on each sublattice, and then laying down valence bonds, i.e. projecting the spin configuration of each pair onto a total-spin singlet, on each pair. If all possible pairings were considered then we would have an overcomplete description, and so we make a final restriction to *non-interleaved* pairings. This final restriction makes use of the order and requires that for any two pairs, one pair lies between the spins which compose the other. Subject to this non-interleaving restriction the basis then becomes complete, although non-orthogonal [7].

The next major task is to achieve a formal description of our chosen basis with which we can work. The method we employ is to construct a *hierarchy* of states from a chosen nearest-neighbour dimer state, by sequentially applying nearest-neighbour spin-singlet projection operators. We choose one of the two nearest-neighbour dimer states and then label the 'gaps' between the singlets with a label, n say. The projection operators that project the two spins either side of the gap onto a total-spin singlet we represent as $\hat{P}_n$, and the projection operators that act on the singlet between the nth and $(n+1)$th gap we represent as $\hat{P}_{n+\frac{1}{2}}$. All the states can then be represented by a sequence of alternating integral half-integral projectors:

$$|I_n, I_{n-1} \ldots I_1, I_0\rangle = \prod_{i_n \in I_n} \hat{P}_{i_n+\frac{n}{2}} \prod_{i_{n-1} \in I_{n-1}} \hat{P}_{i_n+\frac{n-1}{2}} \ldots \prod_{i_1 \in I_1} \hat{P}_{i_1+\frac{1}{2}} \prod_{i_0 \in I_0} \hat{P}_{i_1} |D\rangle \tag{2.1}$$

where $|D\rangle$ is the initial dimer state and I_r are sets of integers. In order to obtain distinct states in our basis, there is a implicit relationship between the sets: the integer i may only be included in I_r if *both* i and $i+1$ are included in I_{r-1}. This restriction ensures that each state is unique. The *order* n is the hierarchy to which the state belongs. We can interpret the states defined in this way quite simply: consider the process of using the singlets to pass down the chain, i.e. start at the leftmost spin, jump to the other spin in its singlet and then pass to the next spin in order, jump to its partner and so on. All spins not encountered in this procedure have been altered by the first hierarchy. We can then consider the leftmost spin as yet uncounted, and use our 'jumping' process to find the spins affected by the second hierarchy but no higher hierarchy. Obviously this argument carries on to all orders.

We employ this basis both as an interpretational aid and as an exact way to perform calculations on finite systems. Although the basis is non-orthogonal, the projection operators, $\hat{P}_\alpha$, are particularly simple in this basis, because they project each state onto only one other state with one out of two matrix elements. Any Hamiltonian which can be decomposed simply into nearest-neighbour projectors is applicable for our method. Obviously all isotropic interactions can be represented in this way, but the representation may not be tractable, as we shall later see.

The variational wavefunctions that we employ are chosen to be translationally invariant, and this restricts our choice. In practice we use

$$|m\rangle = \prod_{n_m} (1 + x_m \hat{P}_{n_m+\frac{m}{2}}) \prod_{n_{m-1}} (1 + x_{m-1} \hat{P}_{n_{m-1}+\frac{m-1}{2}}) \cdots \prod_{n_1} (1 + x_1 \hat{P}_{n_1+\frac{1}{2}}) \prod_{n_0} (1 + x_0 \hat{P}_{n_0}) |D\rangle \tag{2.2}$$

where x_r are variational parameters. Obviously, we are using states of a particular order, although we are not restricting the operation of higher hierarchies to when they make new states. Our current choice is dictated by our ability to control the results rather than the physical intuition of picking useful wavefunctions.

The method of controlling our wavefunctions is straightforward—we reorder commuting transpositions in such a way as to apply the operators from one end of the system sequentially towards the other: each subsequent application is a translated version of the last and so we replace all expectation values by products of *transfer matrices*. Our first task is normalization, and this we ensure by rewriting:

$$\langle m|m\rangle = (D|\ldots\hat{O}_{n-2}\hat{O}_{n-1}\hat{O}_n\hat{O}_{n+1}\hat{O}_{n+2}\ldots|D\rangle \tag{2.3}$$

where

$$\begin{aligned}\hat{O}_n = \prod_{r=0}^{\infty} & \hat{P}_{n+m+\frac{1}{2}+r}(1+x_0\hat{P}_{n+m})(1+x_1\hat{P}_{n+m-\frac{1}{2}}) \\ & \cdots(1+x_{m-1}\hat{P}_{n+\frac{m+1}{2}})(1+x_m\hat{P}_{n+\frac{m}{2}}) \\ & \times(1+x_m\hat{P}_{n+\frac{m}{2}})(1+x_{m-1}\hat{P}_{n+\frac{m-1}{2}}) \\ & \cdots(1+x_1\hat{P}_{n+\frac{1}{2}})(1+x_0\hat{P}_n)\prod_{r=0}^{\infty}\hat{P}_{n-\frac{1}{2}-r}\end{aligned} \tag{2.4}$$

and the initial and final projectors project states onto the chosen dimer, alleviating the necessity for starting out and finishing with the dimer state.

The operator $\hat{O}_n$ projects all pairs of spins before the nth gap onto singlets, permutes the $m+2$ singlets around the nth and $(n+m)$th gap, inclusive of the two which make up the gap, and then projects all subsequent pairs of spins onto singlets. Before application of $\hat{O}_n$ we start out with a state for which the $m+1$ singlets excluding the one before the nth gap are permuted, and after application we end up with the $m+1$ singlets excluding the one after the $n+m$th gap permuted. In order to apply $\hat{O}_n$ we need to be able to represent all total-spin singlet states involving both $m+1$ and $m+2$ singlets. We start out with a particular linear superposition over the states obtainable from the $m+1$ singlets excluding the singlet before the nth gap. We apply the operators on the space of states representing the $m+2$ singlets and then the final projection eliminates the singlet after the $(n+m)$th gap, leading to a state which is a linear superposition over the states obtainable from the $m+1$ singlets excluding the singlet after the $(n+m)$th gap. Obviously, the new superposition is a linear combination of the previous superposition, and so we can represent the operation of $\hat{O}_n$ in terms of a transfer matrix acting on the space of total-spin singlets involving $m+1$ singlet pairs.

In terms of our non-interleaved basis, this procedure is extremely simple, since each state projects down onto only one other state and so we need only describe a vector instead of a matrix in order to represent the total-spin-singlet projection operators, $\hat{P}$. Once we have found our transfer matrix, all we need do is diagonalize it in order to obtain the *relevant* states. An eigenvector yields a state which is preserved by an application of $\hat{O}_n$, and if we start out with a linear superposition over states with different eigenvalues, then the eigenstate with the largest eigenvalue will become exponentially dominant after many applications of the transfer matrix. To normalize our variational state, all we need to do is divide by the relevant power of the chosen eigenvalue.

After having normalized our states, we then need to evaluate energies for relevant Hamiltonians. This is straightforward, but can be numerically expensive for longer-range interactions. The basic idea can be encapsulated by

$$\langle m|\hat{H}_n|m\rangle = \langle D|\ldots\hat{O}_{n-2}\hat{O}_{n-1}\hat{H}_r^n\hat{O}_{n+1+r}\hat{O}_{n+2+r}\ldots|D\rangle \tag{2.5}$$

where $\hat{H}_r^n$ is an operator composed of the operator $\hat{H}_n$ and the operators contained in $\hat{O}_n\hat{O}_{n+1}\ldots\hat{O}_{n+r-1}\hat{O}_{n+r}$ all correctly ordered. Obviously r is the minimum number of the $\hat{O}_n$ which are affected by the operator $\hat{H}_n$. In order to evaluate this type of quantity, we need to be able to represent $m+2+r$ singlets: we start out with the eigenstate of our transfer matrix, projecting all unaffected spin pairs before the represented region onto singlets. We then apply our operator $\hat{H}_r^n$ in the space of $m+2+r$ singlets. We then project out the $r+1$ spin pairs at the end of the affected region and overlap the resulting wavefunction with the dual-space eigenfunction, or equivalently project it onto the original eigenstate.

In practice, we only work with elementary permutations. For example, the operator $\hat{P}_{n+m/2}$ involves interfering with only one $\hat{O}_n$, and so $r=0$ and the calculation is trivial. The operator $\hat{P}_{n+m+1/2}$, however, involves non-commutation with two $\hat{O}_n$s, and hence $r=1$ and we need to represent a slightly larger space. It is also quite easy to represent next-nearest-neighbour interactions, if we remember that the transposition operator is, $\hat{T}_n = 1-2\hat{P}_n$, and that $\hat{T}_n\hat{T}_{n+\frac{1}{2}}\hat{T}_n$ transposes two next-nearest-neighbour spins. Indeed, using these ideas it is clear that any permutation can be rerepresented as a product over total-spin-zero projectors, although r becomes prohibitively large with longer-range permutations.

It should now be clear that performing the variational calculations for the J_1–J_2 model is just a matter of performing strings of projections, diagonalizing the transfer matrix and finally minimizing the resulting energy over the variational parameters, a numerically straightforward (although not easy) sequence of tasks.

As well as the total energy, it is also possible for us to calculate the *long-range* behaviour of some relevant correlation functions. The basic idea is simple: due to our construction, there is a maximum length of singlets which require to be considered. If we consider correlation functions over a length scale much longer than this intrinsic length, then we can immediately deduce the long-range behaviour in terms of eigenvalues of new transfer matrices.

Let us consider the spin–spin correlations initially. We can use long-range permutations to create spin–spin correlations, using the identity, $\hat{T}_{n,n+r} \equiv \frac{1}{2} + 2\boldsymbol{S}_n \cdot \boldsymbol{S}_{n+r}$, for the transposition of the spins on sites n and $n+r$. Since there are no singlets of the relevant length, this transposition must create a pair of singlets stretching over the length r. We can then split up the resulting state by projecting out the spins on the original pairs which made up the stretched singlets. There is a contribution from when they are in a singlet, compensating the factor $\frac{1}{2}$ in the definition of the transposition, together with a contribution where the pair are parallel, i.e. in a triplet configuration. In order to obtain eventual correlations, the product over the $\hat{O}_n$ operators *must* transfer the resulting triplet along the chain to meet its partner. The ratio of the eigenvalues in the total-spin-triplet subspace to that in the total-spin-singlet subspace is therefore directly related to the decay of the spin–spin correlations for our chosen states. To apply this idea, all we need to do is to represent the total-spin-triplet subspace and then find and diagonalize the transfer matrix in this subspace.

Our second family of correlation functions is the so-called ring exchange of cyclic-permutation correlations [8]. We believe that using these correlation functions is the natural way to study the topological excitations in the system. Once again, we go to a range much

longer than the intrinsic length of singlets introduced by our variational parameters. The application of a long-range cyclic permutation will then drag one singlet across the range r. In order to obtain eventual correlations, this additional spin-half must be transferred down the spin chain to its partner. There is an additional subtlety in this problem, since the cyclic exchange does in fact translate one dimer state locally onto the other. The analogue to $\hat{O}_n$ is

$$\begin{aligned}\hat{R}_n = \prod_{r=0}^{\infty} \hat{P}_{n+m+1+r}(1+x_0\hat{P}_{n+m+\frac{1}{2}})(1+x_1\hat{P}_{n+m}) \\ \cdots(1+x_{m-1}\hat{P}_{n+\frac{m+2}{2}})(1+x_m\hat{P}_{n+\frac{m+1}{2}}) \\ \times(1+x_m\hat{P}_{n+\frac{m}{2}})(1+x_{m-1}\hat{P}_{n+\frac{m-1}{2}}) \\ \cdots(1+x_1\hat{P}_{n+\frac{1}{2}})(1+x_0\hat{P}_n)\prod_{r=0}^{\infty}\hat{P}_{n-\frac{1}{2}-r}\end{aligned} \tag{2.6}$$

where we are transferring along an, assumed infinite, region of chain with one dimer state translated by one. The transfer matrix corresponding to $\hat{R}_n$ acts on a subspace which generates all total-spin-half wavefunctions and once again the long-range correlations are controlled by the ratio of the eigenvalues of this transfer matrix to the largest eigenvalue of the total-spin-singlet transfer matrix.

In practice, working with our variational wavefunctions involves several different types of calculations. We need to represent *all* the possible spin configurations for a finite length of spin chain. For the ground state we require to represent the total-spin-singlet subspace, for cyclic-permutation correlations we require to represent the total-spin-half subspace, and for spin–spin correlations we need to represent the total-spin-triplet subspace. In terms of these representations we need to evaluate the transfer matrices for normalization, the passage of a spin-half and the passage of a spin triplet along the chain. In order to calculate these transfer matrices we need to multiply sequentially a set of total-spin-singlet projectors, and so we need to represent these operators in our chosen basis. Diagonalization of these matrices yields the stable spin configuration for the ground state and the decay rate of the correlation functions at long distances. We also need to evaluate the energy of some simple short-range interactions, so that we can minimize this energy over our variational parameters: this evaluation involves further strings of total-spin-zero projectors, represented on rather bigger systems than is required for the normalization.

The fact that cyclic-exchange correlations correspond to the transfer of an extraneous spin-half, while spin–spin correlations correspond to the transfer of an extraneous spin-one, lies behind our physical intuition: we associate long-range cyclic-permutation correlations with low-energy topological excitations and long-range spin–spin correlations with low-energy spin waves.

3. The biquadratic Hamiltonian and its higher-spin generalizations

Comparisons between spin-half and higher spins have been fashionable since the discovery of the 'Haldane gap'. It was soon realized, however, that the inherent simplicity of spin-half means that there are many possible higher-spin generalizations to the Heisenberg model. One such generalization is to the nearest-neighbour total-spin-zero projector Hamiltonian [8]:

$$H = -J\sum_i \hat{P}^0_{i,i+1} \tag{3.1}$$

where $\hat{P}^0_{i,j}$ projects the spin configuration on the ith and jth atoms onto the bit which is a total-spin singlet. In terms of $\hat{S}^2 \equiv (S_i + S_j) \cdot (S_i + S_j)$, this operator can be written as

$$\hat{P}^0_{i,j} = \prod_{m=1}^{2S} \frac{[m(m+1) - \hat{S}^2]}{m(m+1)}. \tag{3.2}$$

For this interaction, only situations for which a nearest-neighbour pair are in a total-spin-singlet are favourable. Due to the rapid decay of the probability that uncorrelated spins are in a singlet as a function of total spin, $1/(1+2S)^2$, and of the probability that anti-parallel spins are in a singlet, $1/(1+2S)$, it soon becomes advantageous to break the translational symmetry and to dimerize the spins. This leads to a quantum mechanical phase of great current interest.

The cause of our interest in these models is that both the spin-half and spin-one variants of these models have been independently solved. The spin-half model is equivalently the Heisenberg model [1] and the spin-one model is equivalently the biquadratic-exchange Hamiltonian [8]. Although the spin-half model is gapless, the spin-one model is already gapped, but with a rather large correlation length of ~ 21 atomic spacings. This gapped state is an excellent test for our variational approach, being such a long-range phenomenon. In our chosen basis, the matrix elements of the Hamiltonian are negative definite, and so the wavefunction is in turn positive definite (non-orthogonality must be considered in this argument). This fact restricts attention to positive values of x_n, and we soon found that the lowest-energy state has monotonically decreasing x_ns. For this model the optimization over x_n is elementary and we can easily 'finite-size' scale.

In figure 1 we have scaled the spin-half and spin-one ground-state energies for both our variational calculations and some Lanczos calculations performed using our non-interleaved basis. The variational calculations are at least an order of magnitude more accurate, but the 'finite-size' scaling is clearly smoother for the Lanczos calculations. At face value the variational calculations look better, but this is rather deceptive: the way in which finite-size Lanczos results scale is strongly indicative of the nature of the system. A comparison between the spin-half and spin-one results clearly indicates a pure power law for the spin-half model but there is clear curvature towards exponential convergence for the spin-one model. These observations are a clear prediction for the different natures of the two systems.

The energy of the system is an important if rather inane quantity to look at. The real interest is in the low-temperature properties of the model which can be deduced from knowledge of the low-energy excitations or usually from knowledge of particular correlation functions of the ground state. In figure 2 we present the correlation lengths deduced from our variational ground states. Although there is some scatter, it is easiest to believe that the spin-half system has an infinite correlation length, whereas the spin-one system has a finite correlation length. Perhaps the best evidence comes from analysing the higher-spin variants of the model, as depicted in the insets: a smooth downward shift of the curves is seen as the spin is reduced, until the intercept with the y-axis crosses the origin. This particular value of spin, S_c say, would correspond to the phase transition where the gap closes. Although it is a rather unphysical parameter, one can use both exact diagonalization and our variational calculations on other than half-integral spins, and make a prediction for S_c, and how the transition is physically effected.

In figure 3 we plot inverse correlation lengths as a function of total spin, S. Lower curves correspond to more parameters, and we are supposed to deduce the function that these curves *limit* to. The most natural picture to us would be a straight line as a function of total spin, striking the x-axis at S_c. Performing an extrapolation at a few values of

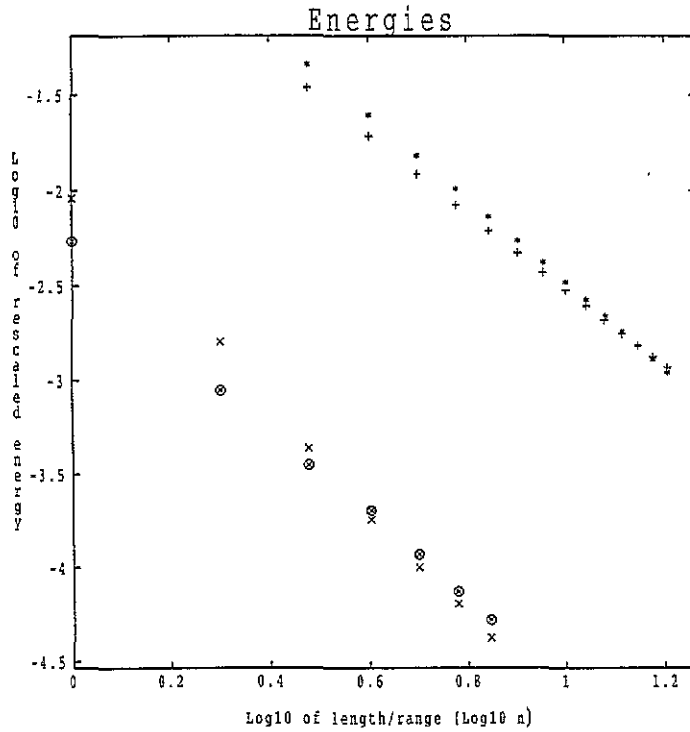

Figure 1. Finite-size scaling calculations for the total energy of the nearest-neighbour Heisenberg model and the spin-one biquadratic-exchange model. In order to assess accuracy, we have plotted $\log_{10}|(\epsilon_n - \epsilon_\infty)/\epsilon_\infty|$ as a function of $\log_{10} n$. The top two graphs show Lanczos exact diagonalization for up to 32 atoms, + for Heisenberg and * for biquadratic, as a function of chain length, n. The bottom two graphs show the current calculations, × for Heisenberg and ○ for biquadratic, as a function of number of variational parameters, n. The current calculations are a couple of orders of magnitude more accurate, but simultaneously less smooth.

total spin, and then performing a linear interpolation yields a prediction of $S_c \sim 0.8$, a not unreasonable possibility. The two types of correlation length yield a consistent result, but the cyclic-permutation correlations yield a more believable prediction.

As well as the total energy, there is also a prediction for the correlation length from the exact calculations on the biquadratic-exchange model [8]. Our results unambiguously suggest that the analytic result does *not* correspond to cyclic-permutation correlations, although it is not inconsistent with spin–spin correlations. This result is a surprise for us.

Our results are clearly consistent with the exact results on these simple models and can be used to make predictions with some degree of confidence.

4. The J_1–J_2 model

In this section we will deal with the spin-half Heisenberg model involving antiferromagnetic interactions of strength J_1 between nearest neighbours and J_2 between next-nearest neighbours. For convenience we have employed the transposition operators to normalize

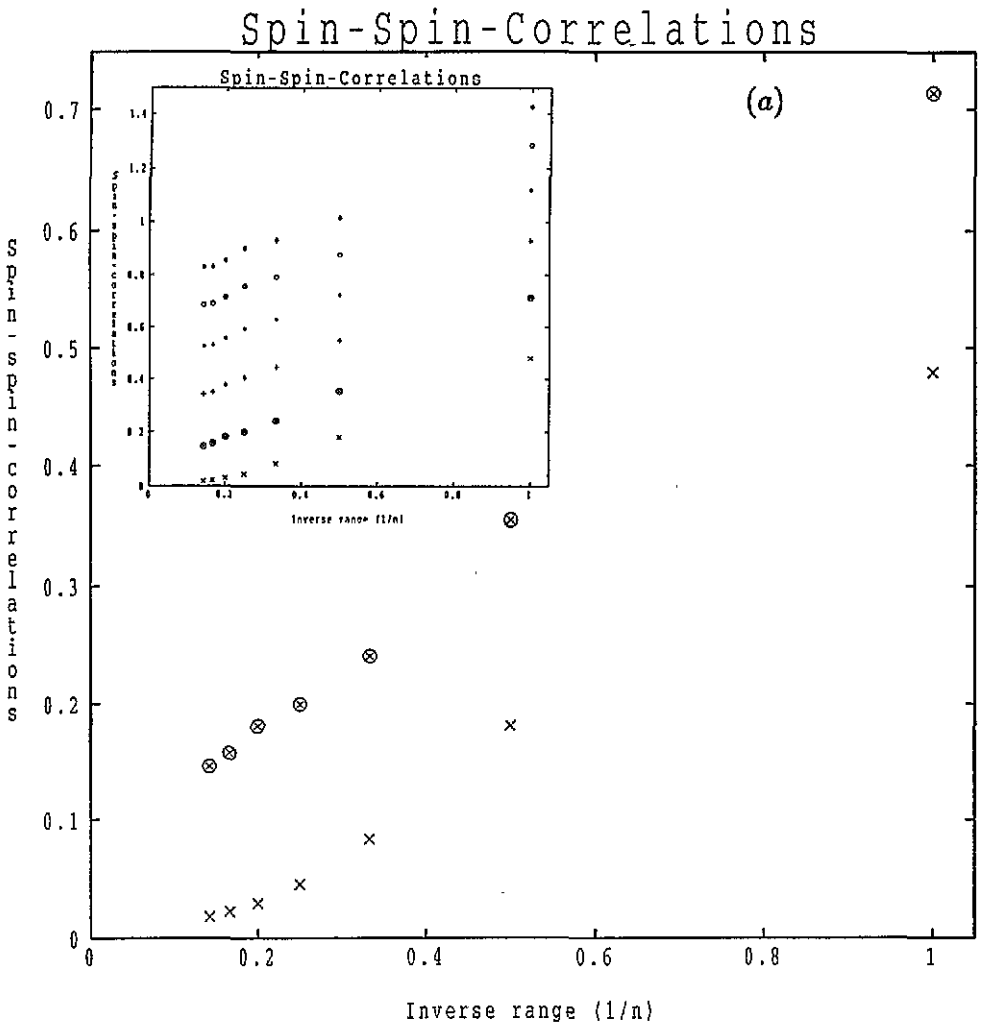

Figure 2. Finite-'size' scaling calculations of the inverse correlation lengths for (a) spin–spin correlations and (b) cyclic-permutation correlations, as a function of inverse 'size'—for the current calculations the number of independent variational parameters. The total-spin-zero projector is the Hamiltonian, and we looked at $S = 0.5$ and 1 (1.5 2 2.5 3 inset), as we progress up the figure. The spin-half model appears to yield a divergent correlation length, whereas the spin-one model does not.

out energies:

$$H = J_1 \sum_i \left[\frac{1}{2} + 2S_i \cdot S_{i+1}\right] + J_2 \sum_i \left[\frac{1}{2} + 2S_i \cdot S_{i+2}\right] \tag{4.1}$$

where $\hat{T}_{i,j} = \frac{1}{2} + 2S_i \cdot S_j$ transposes the two spins at sites i and j. With this choice of normalization the dimer solution has zero energy.

Our approximation scheme is based around a chosen dimer state. Since when $2J_2 = J_1$ this state is an exact solution, we might expect our results to *improve* as J_2 is increased.

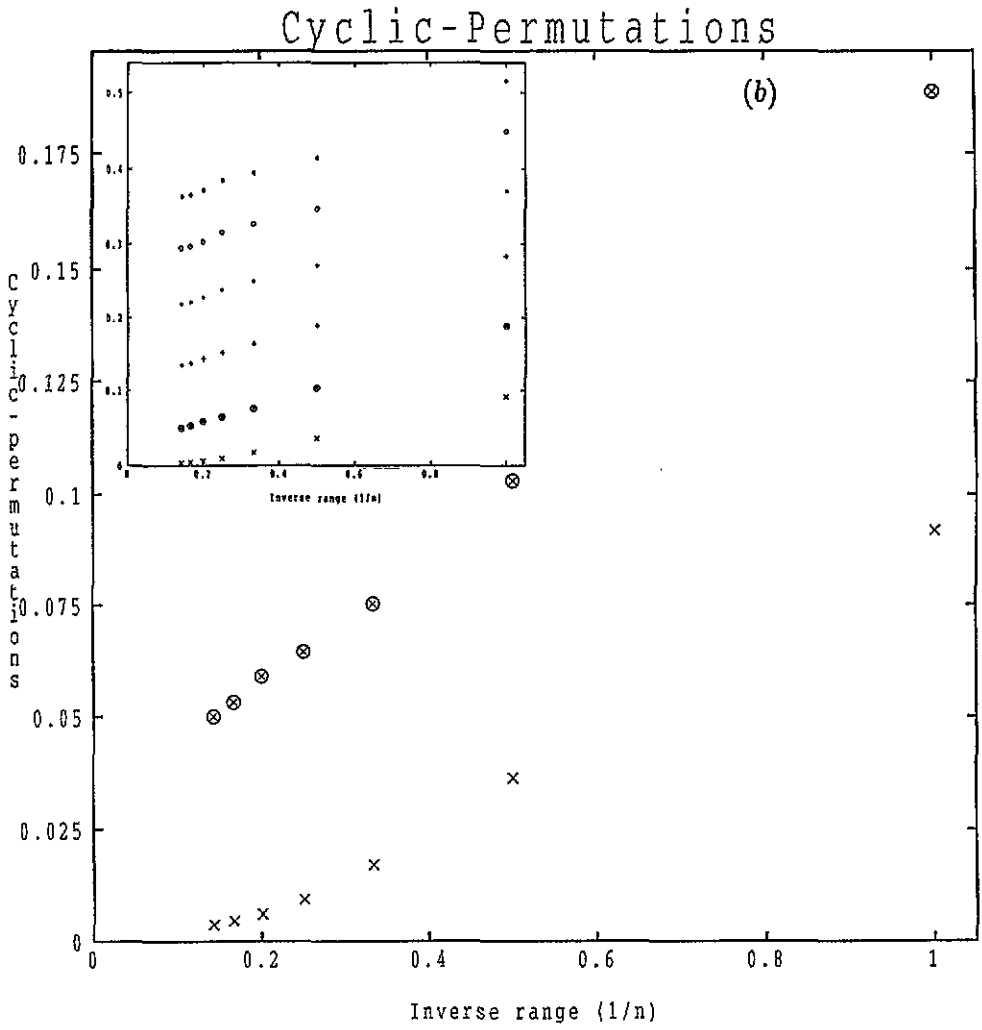

Figure 2. (Continued)

Our results are presented in figure 4. Since exact results are not known as J_2/J_1 is varied, we have made estimates for the eventual ground-state energies. Our method of estimating the energy was to use the *smoothness* of the exact diagonalization results, and to make these curves appear 'natural', usually linear. The relative positions of the curves do not depend greatly upon this particular choice of energy, ϵ_∞, although their perceived smoothness does. Unlike the previous projector calculations, the results are very messy, involving a collection of low-energy states with quite different parametric descriptions. Although the results are quite accurate, the scaling is not very smooth, since the states are continuously changing their structure. We should also point out that our search for low-energy solutions has been by no means exhaustive, and there may well be solutions of our projected form that we have not encountered.

The correlation functions are much more interesting: the cyclic-permutation correlations are of *much* longer range than the spin–spin correlations, as is to be expected if the corresponding topological excitations control the phase transition. The spin–spin

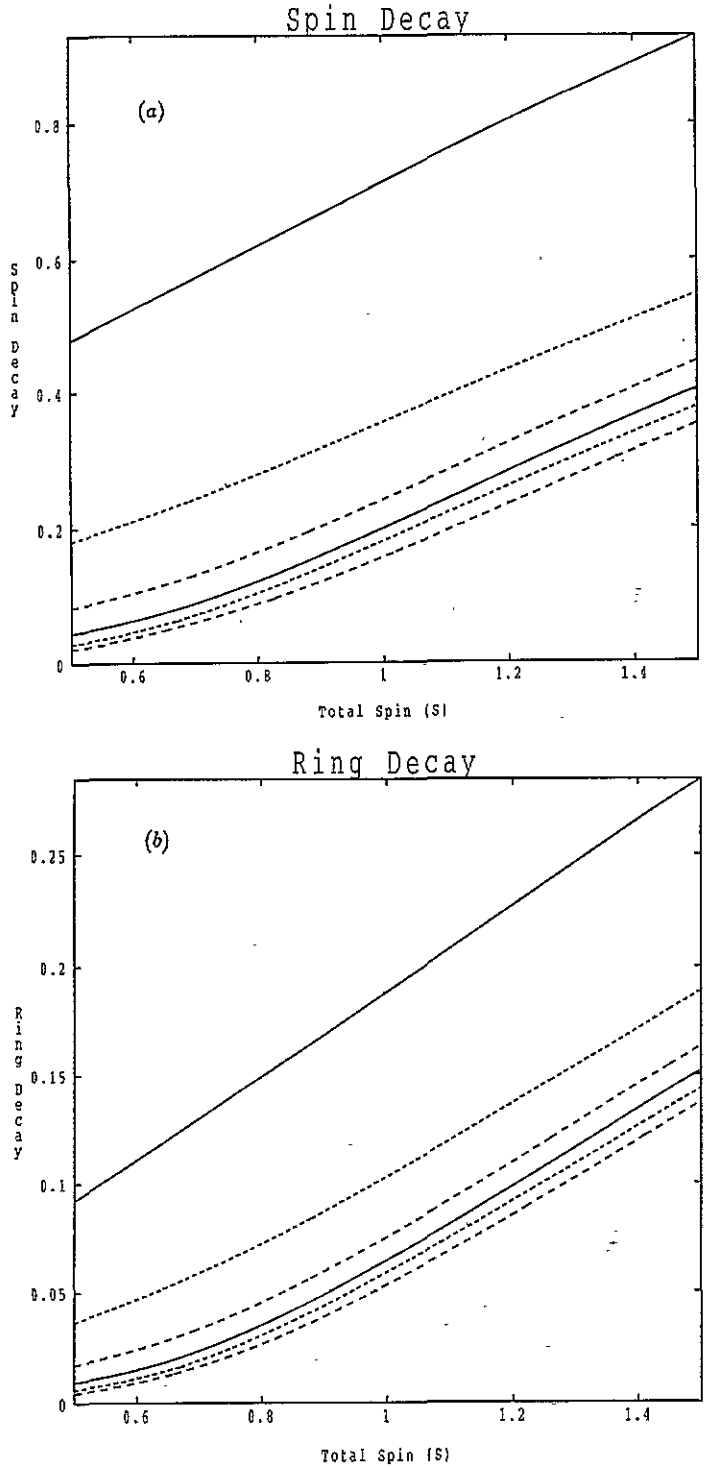

Figure 3. Finite-'size' scaling calculations of the inverse correlation lengths for (a) spin–spin correlations and (b) cyclic-permutation correlations, as a function of total spin, S, for a range of values including the phase transition. The sequence of calculations progressing down the figure involve sequentially including an additional variational parameter.

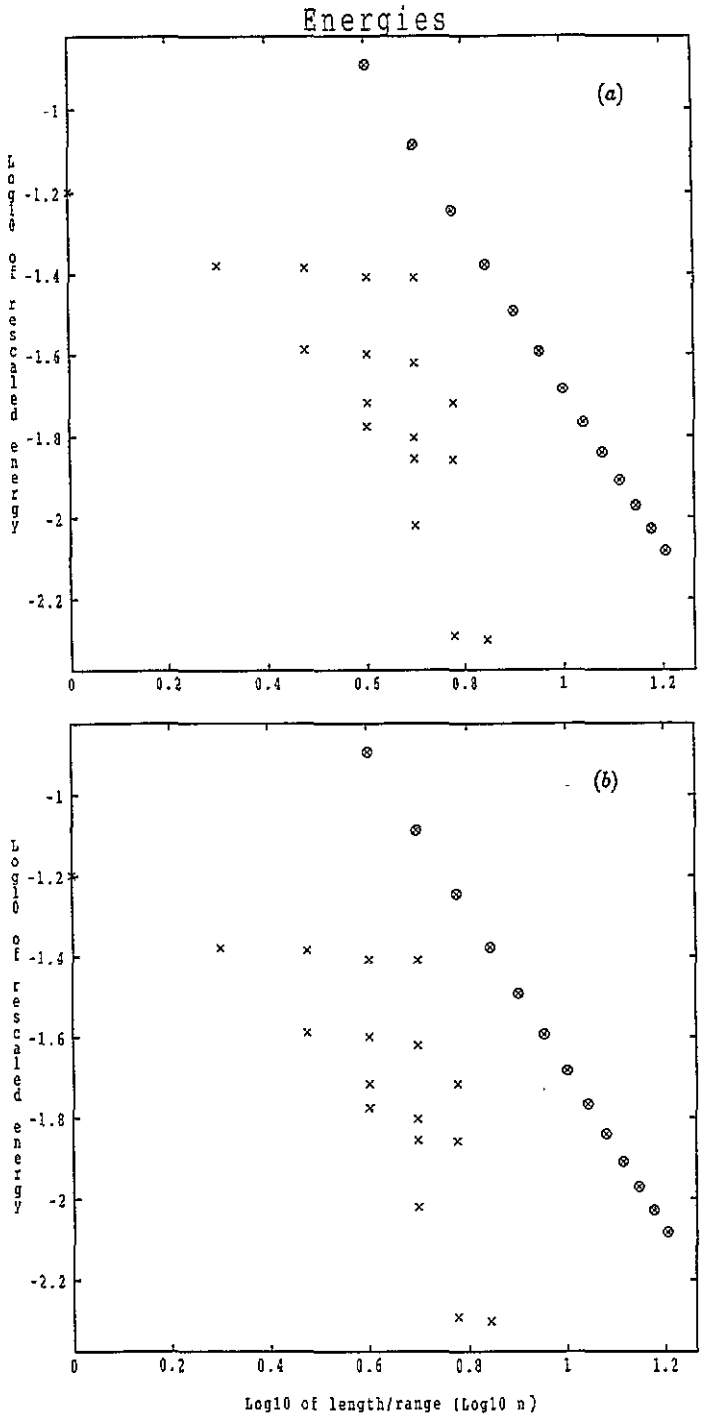

Figure 4. Finite-size scaling calculations for the total energy of the J_1–J_2 Heisenberg model for the cases (a) $J_2/J_1 = 0.1$, (b) $J_2/J_1 = 0.2$, (c) $J_2/J_1 = 0.3$, (d) $J_2/J_1 = 0.4$. In order to assess accuracy, we have plotted $\log_{10}|(\epsilon_n - \epsilon_\infty)/\epsilon_\infty|$ as a function of $\log_{10} n$, we have had to estimate the exact answer, and we used (a) $\epsilon_\infty = -0.6015$, (b) $\epsilon_\infty = -0.4340$, (c) $\epsilon_\infty = -0.2722$, (d) $\epsilon_\infty = -0.1213$. The top graphs show Lanczos exact diagonalization for up to 32 atoms, and the bottom graphs show a collection of low-energy states from our current analysis.

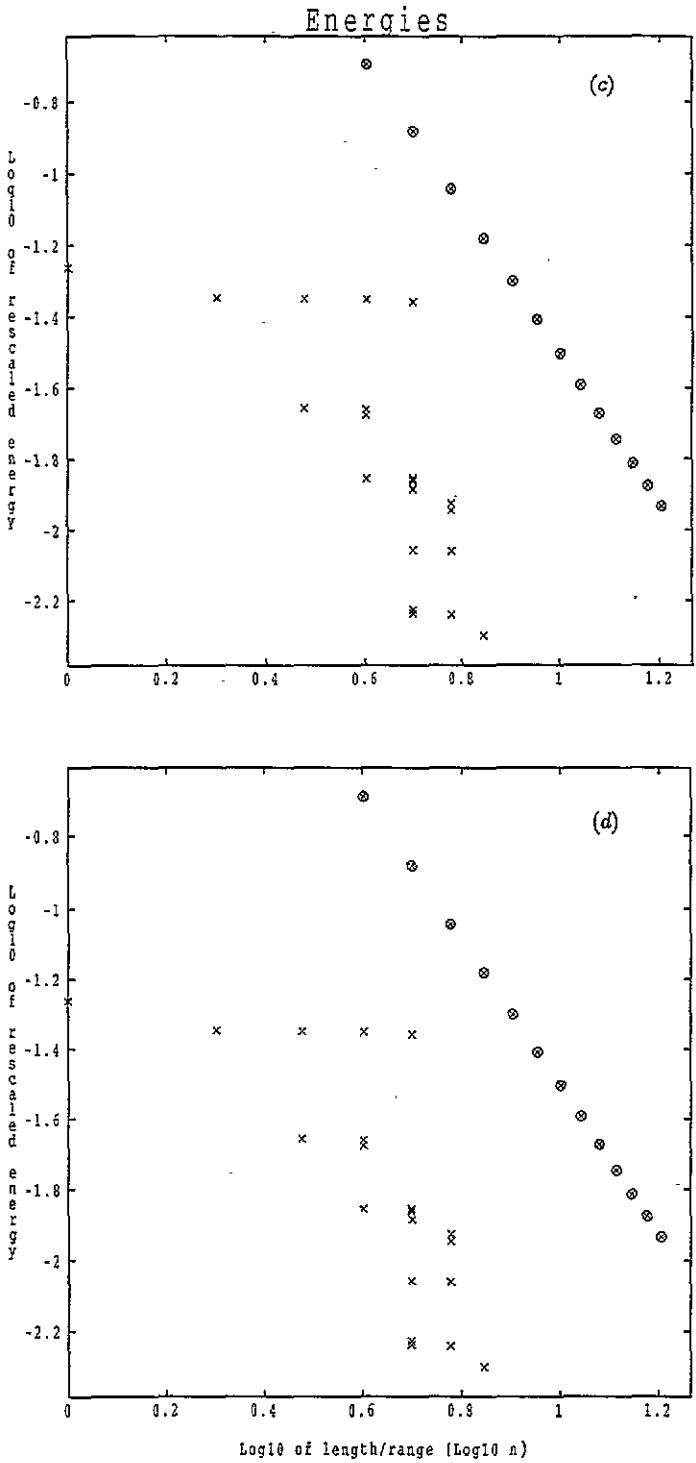

Figure 4. (Continued)

correlations vary more dramatically, due to the divergence present in the dimer state which occurs when $2J_2 = J_1$. It is clear that the phase transition will be easier to predict from the ring-exchange correlations.

We plot the inverse correlation lengths for our lowest-energy calculations in figure 5. The discontinuities are caused by changes in the characteristics of the lowest-energy solution, and clearly constitute quite important effects. If we presume a *non-linear* dependence on inverse correlation length on the parameter J_2/J_1, then the correlation functions predict that the transition should occur somewhere around $4J_2 = J_1$, as predicted by the classical theory. The scaling is not clear, and the result predicted could be as large as $J_2 = 0.4J_1$.

The assumption underlying the current investigation is that the topological excitations control the phase transition and these excitations can be probed using the cyclic-permutation correlations. One important consideration is that one might expect the cyclic-exchange correlations to be *maximal* when the phase transition occurs. There is no evidence for the correlation length achieving a maximum away from $J_2 = 0$. However, it should be borne in mind that the calculations are much more accurate when $J_2 = 0$, and so the correlation length may be of longer range for this reason.

The absolute values of the correlation lengths are also worthy of note, since if these lengths were to be finite for $J_2/J_1 = 0.3$, for example, then the associated cyclic-permutation correlation length would need to be much longer than 30 atoms—very difficult to pick up with any numerical technique.

The final fact to point out in this section is that the current results are *not* what we would have naively expected: although the dimer becomes the exact solution in the limit $2J_2 \mapsto J_1$, the corrections inherent to our projection scheme do not smoothly correct this state and we are left with a quite unnatural description of the ground state in the vicinity of this point. The theory makes predictions, but the 'systematic' improvements are not easy to scale. We believe that this defect is the most severe for our technique, and will ultimately restrict its applicability.

5. The ladder geometry

In this section we consider the spin-half Heisenberg model on the so-called 'ladder geometry' of two lines of parallel atoms. Unlike the previous two geometries, the ladder geometry has two atoms per unit cell. If we denote atoms along one 'rail' of the ladder by S_i and along the other rail by T_i, where i is a label for the 'rungs' of the ladder, then this Hamiltonian may be written as

$$H = J_{\parallel} \sum_i \left[S_i \cdot S_{i+1} + T_i \cdot T_{i+1} \right] + J_{\perp} \sum_i S_i \cdot T_i \tag{5.1}$$

where $J_{\parallel}$ is the matrix element for bonds parallel to the rails and $J_{\perp}$ is the matrix element for the bonds across the rungs. Since we start out with a dimer state, we are already in a 'two atom per unit cell' situation. Instead of being a degeneracy, for the ladder geometry, the two possible choices of dimer are crucial to the current theoretical discussion: there are two types of ground state to the ladder geometry, and hence a phase transition between them, but where does this transition occur? For our technique, the two possible choices of dimer correspond to the two possible ground states.

We have elected to order the atoms by nearest neighbours, in the 'snake' connectivity. This choice is required on account of the inherent reflection symmetries in our variational wavefunctions. There are two types of bond: $J_1 = J_{\parallel}$ parallel to the ladder and $J_2 = J_{\perp}$

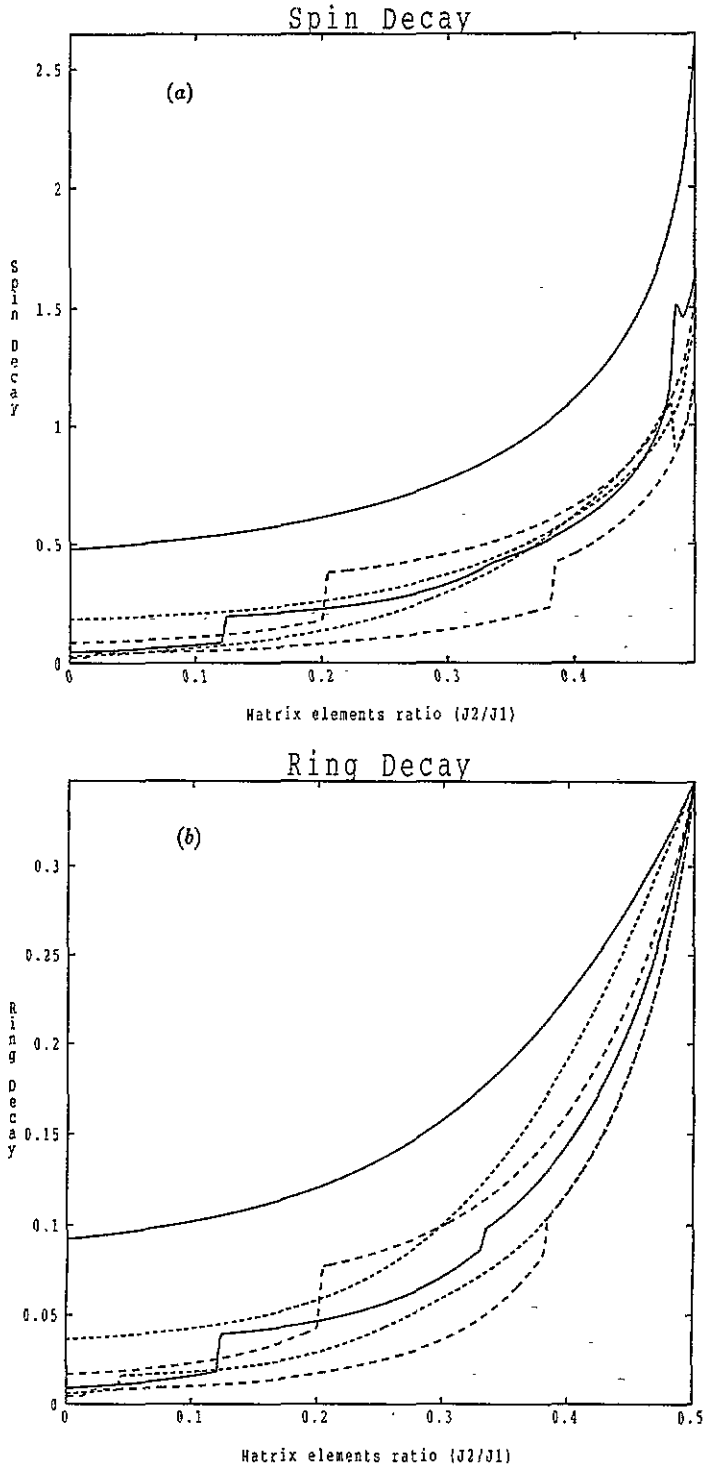

Figure 5. Finite-'size' scaling calculations of the inverse correlation lengths for (a) spin–spin correlations and (b) cyclic-permutation correlations, as a function of J_2/J_1 for a range of values including the phase transition. The sequence of calculations progressing down the figure (at the left edge) involve sequentially including an additional variational parameter.

for the rungs. One dimer state solves the limit $J_\perp \gg J_\parallel$, since a singlet is laid down on each of the $J_\perp$-bonds. In this limit there is a gap to triplet excitations. In the opposing limit $J_\parallel \gg J_\perp$, the ground state involves two uncorrelated Heisenberg ground states along the two rails of the ladder. This state is gapless, involving topological excitations on either rail. The second dimer state involves laying down singlets on *half* of the $J_\parallel$ bonds, and so makes a suitable starting point for the gapless phase.

Similarly to in the case of the projector Hamiltonian, but unlike in that of the J_1–J_2 model, the low-energy parametrization for our technique is straightforward. The basic trick is to alternate variable x_ns with the specific choice of $x_n = -2$. Since, $1 - 2\hat{P}_n = \hat{T}_n$ is a transposition operator, the choice $x_n = -2$ corresponds to an infinite product of elementary transpositions. The transpositions are used to 'swap' the spin correlations between the two rails of the ladder, and the intermediate projectors introduce correlations *along* the rails, alternating between the two halves of the $J_\parallel$-bonds. In the two limits, $x_n = -2$ is *exact*, but for the general case the basic pattern is 'similar' and easy to find because of this. Any solution to the nearest-neighbour Heisenberg model can be constructed concurrently on both rails of the ladder, by alternating the x_ns of the chain solution with $x_n = -2$, for example.

We have performed calculations on the ladder geometry analogous to those that we did for the previous geometries. In figure 6 we plot the energies, once again showing that our variational wavefunctions are competitive and appear to converge systematically to the exact solution. The sequence of calculations is quite instructive: there is a small region of stability for the phase based upon independent rails in the vicinity of $J_\perp \mapsto 0$. As the number of parameters increases, so this region of stability shrinks. Obviously, by projecting one dimer state onto the other, we can turn one type of state into the other. This guarantees that there is an alternation in our calculations as $J_\perp \mapsto 0$, and then our calculations suggest that the state based upon correlations between rails is stabilized for $J_\perp > 0$.

For the current geometry, cyclic permutations are not relevant, and show only short-range correlations across the entire range of parameters, as one would expect.

The inverse correlation lengths are scaled in figure 7. It is easiest to believe that the gap opens up immediately that $J_\perp$ is made finite. This is in complete agreement with the deductions made from other calculations [9]. We also see that as one would expect, the state with correlations along the rails gains from correlating the two rails together, yielding classical magnetic energy. The physical point is that for this low-dimensional system, quantum mechanics dominates, and there is more energy in quantum mechanical fluctuations than in classical order.

6. Conclusions

Using our complete but non-orthogonal basis of total-spin singlets [7], we have developed a systematic variational approximation scheme for one-dimensional Heisenberg models and their correlation lengths. We have applied our scheme to the total-spin-zero projector Hamiltonian as a function of total spin, S, to the J_1–J_2 Heisenberg model as a function of J_2/J_1, and also to the ladder geometry as a function of $J_\perp/J_\parallel$. We find evidence for the phase transitions between gapped and gapless states in these models, yielding a prediction of $S_c \sim 0.8$, a rather poorer 'guestimate' of $J_2^c \sim J_1^c/4$, and evidence that $J_\perp^c \mapsto 0$.

We have analysed the long-range properties of cyclic permutation correlations and spin–spin correlations and we find that cyclic-permutations control the phase transitions in the projector Hamiltonians and the J_1–J_2 model, but that spin–spin correlations control the ladder geometry. This is exactly as physically expected.

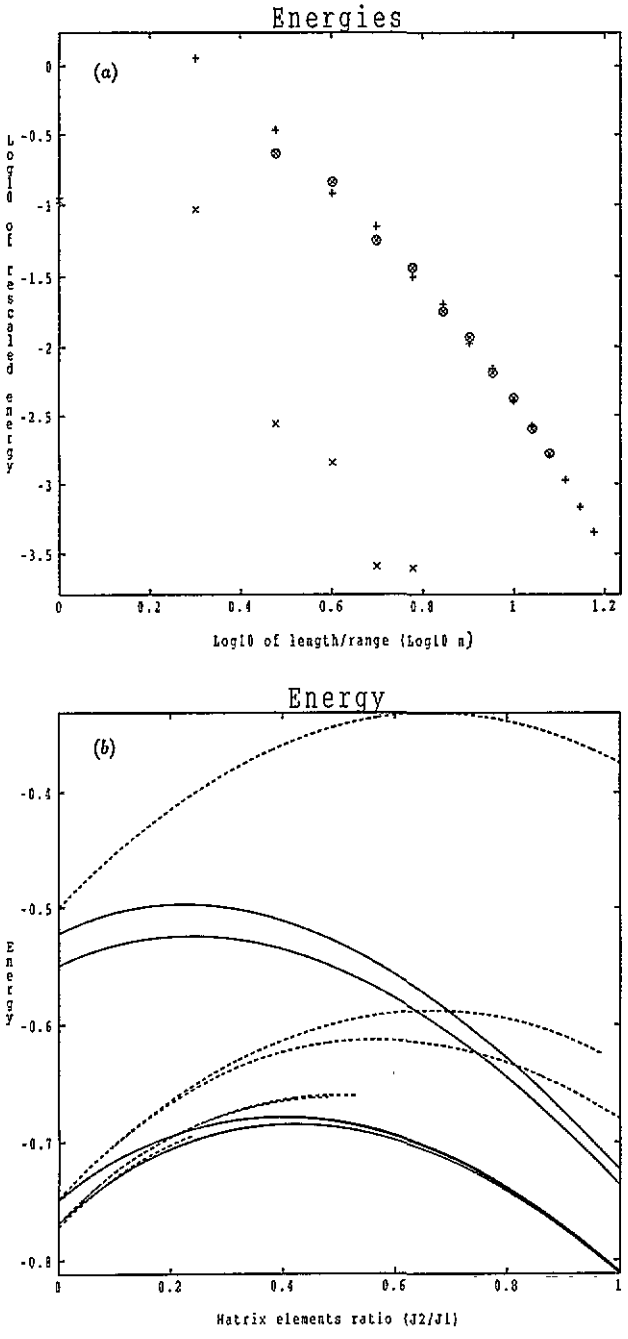

Figure 6. Finite-size scaling calculations for the total energy of the ladder geometry. (a) Comparison of $\log_{10}|(\epsilon_n - \epsilon_\infty)/\epsilon_\infty|$ as a function of $\log_{10} 1/n$, we have had to estimate the exact answer, and used $\epsilon_\infty = -0.812\,17$ (we use projector Hamiltonians not Heisenberg-like ones). The top two curves show Lanczos diagonalization, with ⊗ indicating use of Mobius boundary conditions and + indicating use of independent rails. The bottom curve shows our projector technique. (b) Overlay of total energies of states with increasing numbers of variational parameters, as a function of $J_\perp/J_\parallel$. The full lines involve the dimers on the rungs, and the dotted lines involve the dimers along the rails. Note that the points at which subsequent dotted and full lines cross converge towards $J_\perp = 0$.

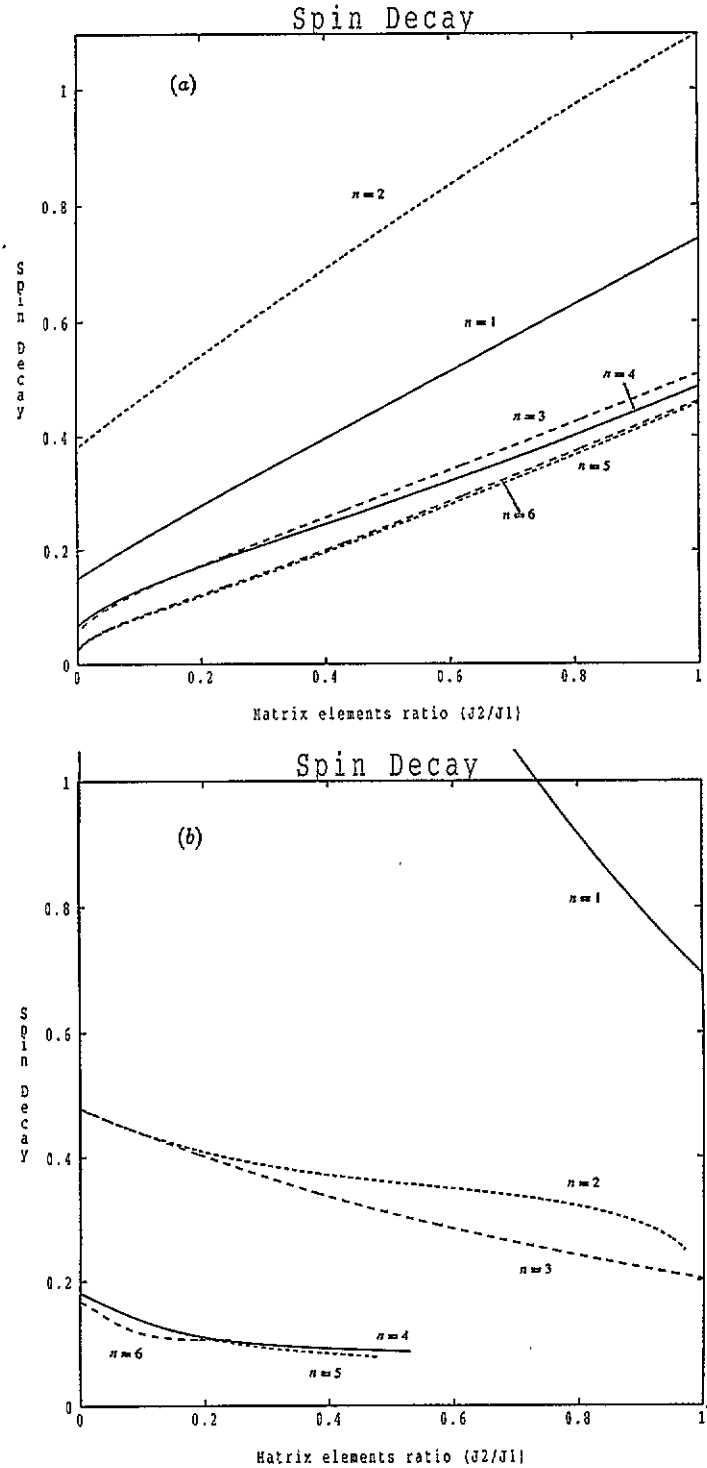

Figure 7. Finite-'size' scaling calculations of the inverse spin–spin correlation lengths for (a) the states with dimers on the rungs and (b) the states with dimers along the rails. The first calculation suggests a divergent correlation length only at $J_\perp = 0$, while the second calculation shows that the correlation length increases as the rails become coupled.

The technique itself is a transfer-matrix calculation: we create states via a sequence of translationally invariant nearest-neighbour projections from a reference dimer state. The action of our projection operators is controlled in a small finite total-spin-singlet subspace, for which the projections map each original basis state onto only one other. The transfer matrices are a product of a finite number of these projections in our finite subspace, and are therefore easy to evaluate. The behaviours of the normalization and correlation functions are then controlled by the eigenvalues of these transfer matrices. The states we choose are parametrized by a sequence of numbers, which are chosen to minimize the energy of the state. Unfortunately, this final optimization problem is sophisticated, and unless one can deduce the likely form of the low-energy solutions, there is no easy way to perform the optimization. We are currently limited by our skill at dealing with this final optimization problem. The calculations are variational and systematic. We easily obtain comparable accuracy with exact-diagonalization calculations, and find the correlation lengths much easier to evaluate.

We have provided some numerical estimates of quantities found using exact analysis [8], and although we get good agreement with energies, our correlation lengths do not unambiguously agree (when finite). We find a correlation length for the spin-one biquadratic-exchange Hamiltonian that is of longer range than is predicted [8], although this could easily be due to the fact that we are looking at different correlation functions—viz cyclic permutations rather than spin–spin correlations.

Our results are in general agreement with those from other styles of calculation, and should be seen as an independent approach. Currently, we have only investigated a single type of variational state. There is much room for improvement in the classes of wavefunction chosen for investigation.

References

[1] Bethe H A 1931 *Z. Phys.* **71** 205
[2] Fadeev L D and Takhtajan L A 1981 *Phys. Lett.* **85A** 375
[3] Majumdar C K and Ghosh D K 1969 *J. Math. Phys.* **10** 1338
[4] Long M W and Hayward C A 1994 *J. Phys.: Condens. Matter* **6** 2773
[5] Schultz H J 1991 *Int. J. Mod. Phys.* B **5** 57
[6] Jordan P and Wigner E 1928 *Z. Phys.* **47** 631
[7] Temperley H N V and Lieb E H 1971 *Proc. R. Soc.* A **322** 251
Bondeson S R and Soos Z G 1980 *Phys. Rev.* B **22** 1793
Long M W and Siak S 1993 *J. Phys.: Condens. Matter* **5** 5811
[8] Barber M N Batchelor M T 1989 *Phys. Rev.* B **40** 4621
Klumper A 1990 *J. Phys. A: Math. Gen.* **23** 809
[9] Barnes T, Dagotto E, Riera J and Swanson E S 1993 *Phys. Rev.* B **47** 3196
Dagotto E, Riera J and Scalapino D J 1992 *Phys. Rev.* B **45** 5744
Strong S P and Millis A J 1992 *Phys. Rev. Lett.* **69** 2419
Rice T M, Gopalan S and Sigrist M 1993 *Europhys. Lett.* **23** 445